Refractive Index Change Analysis in a High-Power Yb-doped Double-Clad Fiber Laser

Elbis Santos Cardoso
University of São Paulo
São Paulo, Brazil
elbis@usp.br

Ricardo Elgul Samad
IPEN-CNEN/SP
São Paulo, Brazil
orcid.org/0000-0001-7762-8961

Cláudio Costa Motta
University of São Paulo
São Paulo, Brazil
orcid.org/0000-0002-2508-7320

2021 SBFoton International Optics and Photonics Conference (SBFoton IOPC) | 978-1-6654-1948-2/21/$31.00 ©2021 IEEE | DOI: 10.1109/SBFOTONIOPC50774.2021.9461981

***Abstract*—An analytical investigation of the refractive index behavior of an ytterbium-doped optical fiber silica glass as a function of the core-clad temperature, upper-level population laser density, and pumping signal intensity is presented in this paper. For the substantiation of the investigation, three fundamental expressions were used, which describe the changes in the refractive index due to these physical phenomena in the laser medium. The model was evaluated considering a 500 W steady state fiber laser, operating in a two-end pumped configuration.**

***Index Terms*—High-power fiber laser, ytterbium-doped optical fiber, refractive index change.**

I. Introduction

High-power Yb^{3+}-doped double-clad fiber lasers (YDCFL) have been widely used in many industrial and scientific applications due to their excellent advantages, such as high brightness, high efficiency, compactness and beam quality when compared to traditional gas and solid state lasers.

Analitycal descriptions of high power YDCFLs in forward and bidirectional pump modes, delivering above 1 kW of output power, in continuous wave regime, have been reported by several authors [1]. Moreover, the thermal problem has been described by M. Karimi [2] and J. Li [3], including heat transfer mechanisms, such as, conduction, convection and radiation. Those results have shown that the two-end pumping in YDCFL can achieve a more uniform temperature distribution in both axial and radial directions of the fiber when compared to the forward-pumped mode, according to experiments [2, 3]. However, those papers didn't include an analysis of the refractive index changes. The understanding of these changes are relevant to control the beam optical quality. In this context, and in order to evaluate the contribution of temperature, the upper-level laser population density, and the pumping signal intensity, on the refractive index in the core-cladding bulk of the YDCFL, an analytical study is presented.

This paper is organized as follows: Section 2 presents an analysis of the refractive index behavior as a function of fiber temperature, upper-level laser atomic population density, and the pumping signal intensity (both radial and axial directions). The results and discussion are presented in Section 3. Finally, the conclusion is presented in Section 4.

II. Refractive index changes in a YDCFL

A. Dependence of the refractive index with fiber temperature

Refractive index changes $\Delta n_{core/clad}(r,z)$ due to the fiber temperature variations, $\Delta T(r,z)$, occur in the radial (r) and axial (z) directions, because the temperature $T(r,z)$ within the fiber depends on the heat flow $Q(z)$, as a consequence of the scattering losses. According to Yan [4], the equations that describe the temperature variation in the core-cladding region of the optical fiber are given by (1) and (2), shown in the next page, where r_{core} and r_{clad} denote the fiber core and cladding radii, respectively, and h_c and κ are the convective and conductive coefficients, respectively. As shown in (3), the refractive index variation in the fiber core-clad region depends on the temperature changes and the thermo-optical coefficient $\beta = \frac{dn}{dT} = 1.2 \times 10^{-5} K^{-1}$ for silica glass [5].

$$\Delta n_{core/clad}(r,z) = \frac{dn}{dT} \Delta T_{core/clad}(r,z) \tag{3}$$

Substituting (1) and (2) into (3), provides (4) and (5) (in the next two pages) that describe the refractive index variation in the optical fiber core-clad region due to the temperature. The heat flow $Q(z)$ is defined by (6), according [2,3], where $\alpha(z) = \alpha_\alpha(z) + \alpha_s$, $\alpha_\alpha(z)$ is the absorption coefficient, which can be expressed as $\alpha_\alpha(z) = \Gamma_p[(\sigma_s^e + \sigma_s^a)N_2(z) - \sigma_s^a N_{Yb}]$, S is the quantum efficiency, whose theoretical value is $\frac{\lambda_s}{\lambda_p}$, α_s represents the scattering loss coefficient of light signal. λ_s and λ_p denote the laser and pump wavelengths, $P_p(z)$ is the pump power, given by $P_p(z) = P_p^+(z) + P_p^-(z)$, and A_{eff} is the effective core area.

$$Q(z) = \frac{\alpha(z) P_p(z)(1-S)}{A_{eff}} \tag{6}$$

B. Dependence of the refractive index with the upper-level population density

The behavior of the refractive index in the core of the Yb^{3+}-doped optical fibers as a function of the upper-level population density in the axial direction, considering the Kramers-Kronig effect, given by $\Delta kk = 1.2 \times 10^{-30} m^3$ for silica glass, is described by (7) and (8) [1, 5]. In (8), $P_p^+(z)$ and $P_p^-(z)$ represent the forward and backward pump powers along the fiber, respectively. $P_s^+(z)$ and $P_s^-(z)$ represent the forward

978-0-7381-2418-6/21/$31.00 ©2021 IEEE

$$\Delta T_{core}(r,z) = \frac{Q(z) r_{core}^2}{4\kappa}\left[1 - \left(\frac{r}{r_{core}}\right)^2 + 2\ln\left(\frac{r_{clad}}{r_{core}}\right) + \frac{2\kappa}{r_{clad} h_c}\right], 0 \le r \le r_{core} \quad (1)$$

$$\Delta T_{clad}(r,z) = \frac{Q(z) r_{core}^2}{2\kappa}\left[\frac{\kappa}{r_{clad} h_c} - \ln\left(\frac{r}{r_{core}}\right)\right], r_{core} < r \le r_{clad} \quad (2)$$

$$\Delta n_{core}(z) = \frac{dn}{dT}\left\{\frac{Q(z) r_{core}^2}{4\kappa}\left[1 - \left(\frac{r}{r_{core}}\right)^2 + 2\ln\left(\frac{r_{clad}}{r_{core}}\right) + \frac{2\kappa}{r_{clad} h_c}\right]\right\} \quad (4)$$

and backward signal powers along the fiber, respectively. h is the Planck constant, v_s and v_p are the frequencies of the laser and pumping signals, respectively. N_{Yb} is the density of Yb^{3+} and $N_2(z)$ is the upper-level laser population density. σ_p^a and σ_p^e are the absorption and emission cross sections at the pump wavelength, respectively, σ_s^a and σ_s^e are the absorption and emission cross sections at the signal wavelength, respectively. τ_2 is the lifetime of Yb^{3+}. Γ_s and Γ_p are the power filling factors for the signal and pump, respectively.

$$\Delta n_{core}(z) = [\Delta kk]\, N_2(z) \quad (7)$$

C. Dependence of the refractive index with the pumping signal intensity

According to Digonnet [6], the refractive index dependence on the pumping signal $P_p(z)$ is:

$$\Delta n_{core}(z) = q f_{12} \lambda_{12} N_{Yb} g_{12}(\omega_s)\left[\frac{\frac{P_p(z)}{A_{eff} I_{p,sat}}}{1 + \frac{P_p(z)}{A_{eff} I_{p,sat}}}\right] \quad (9)$$

$$g_{12}(\omega_s) = \frac{1}{\pi}\frac{2\omega_{12}(\omega_{12}^2 - {\omega_s}^2)}{(\omega_{12}^2 - {\omega_s}^2) + (\delta\omega_{12}\omega_s)^2} \quad (10)$$

$$I_{p,sat} = \frac{h v_p}{(1 + g_1/g_2)\sigma_p \tau_2} \quad (11)$$

where $q = e^2 K/8nm_e\varepsilon_0 c$ is a material constant, e and m_e are the charge and the mass of the electron, respectively. K is the Lorentz correction factor, given by $K = (n^2+2)^2/9$. n is the fiber core refractive index, c is the speed of light in vacuum, ε_0 is the electric permittivity of vacuum. f_{12} is the oscillator strength of the transition. $g_{12}(\omega_s)$ is the lorentzian lineshape, where ω_{12} is the transition frequency between the ground state (level 1) and an excited state (level 2). ω_s is the angular frequency of the laser signal, and $\delta\omega_{12}$ is the full width at half maximum (FWHM) of the transition, considering $\delta\lambda_{12} = 0.02\lambda_{12}$ according [6], and $I_{p,sat}$ is the pump saturation intensity of the transition, where g_1/g_2 is the degeneracy ratio of levels 1 and 2. The other parameters of (9) are given in Table I. It is assumed that the intensity levels in the structure are maintained below the critical value at which distortions caused by optical nonlinear effects become relevant.

III. Results and Discussion

The parameters used in the analytical formulation are shown in Table I [3].

TABLE I
FIBER AND THERMAL PARAMETERS USED FOR SIMULATING

Symbol	Parameter	Value
L	Fiber length	$12m$
n	Core refractive index	1.47
A_{eff}	Effective core area	$900 \times 10^{-12} m^2$
$P_p^+(z)$	Forward pump power	$500W$
$P_p^-(z)$	Backward pump power	$500W$
λ_s	Signal wavelength	$1.060\mu m$
λ_p	Pump wavelength	$976\mu m$
Γ_s	Signal power filling factor	0.82
Γ_p	Pump power filling factor	0.01
N_{Yb}	Yb^{3+} concentration	$6 \times 10^{25} m^{-3}$
τ_2	Radiative lifetime	$1ms$
σ_p^a	Pump absorption cross section	$6 \times 10^{-25} m^{-2}$
σ_p^e	Pump emission cross section	$2.5 \times 10^{-27} m^{-2}$
σ_s^a	Signal absorption cross section	$1.40 \times 10^{-27} m^{-2}$
σ_s^e	Signal emission cross section	$2.0 \times 10^{-25} m^{-2}$
α_p	Scattering loss coefficients of pump light	$3.0 \times 10^{-3} m^{-1}$
α_s	Scattering loss coefficient of signal light	$5.0 \times 10^{-3} m^{-1}$
R_1	First reflector	0.98
R_2	Second reflector	0.04
κ	Heat conductive coefficient.	$1.38W \cdot m^{-1} \cdot K^{-1}$
h_c	Convective coefficient	$10W \cdot m^{-2} \cdot K^{-1}$
δ	Stefan Boltzmann constant	$5.67 \times 10^{-8} W(m^2 K^4)^{-1}$
ε	Emissivity	0.95
T_c	Ambient temperature	$298K$

At $z = 0$ and different radii values, Table II shows the refractive index as a function of temperature, the upper-level population density and the pumping signal.

Analyzing the results of the refractive index changes as a function of the core-cladding temperature, shown in Table II and in Fig. 1, it is possible to observe that, in the steady state regime the maxima of the refractive index variation are achieved at the ends of the fiber ($z = 0$ and $z = L = 12m$), considering the center of the fiber ($r \approx 0$). Furthermore, the minimum value is achieved at the middle of the fiber, for the maximum radius $r = 400\mu m$.

$$\Delta n_{clad}(z) = \frac{dn}{dT}\left\{\frac{Q(z)r_{core}^2}{2\kappa}\left[\frac{\kappa}{r_{clad}h_c} - \ln\left(\frac{r}{r_{core}}\right)\right]\right\} \tag{5}$$

$$N_2(z) = N_{Yb}.\frac{\left(\frac{\Gamma_p}{h\upsilon_p A}\right)\sigma_p^a[P_p^+(z)+P_p^-(z)] + \left(\frac{\Gamma_s}{h\upsilon_s A}\right)\sigma_s^a[P_s^+(z)+P_s^-(z)]}{\left(\frac{\Gamma_p}{h\upsilon_p A}\right)(\sigma_p^a+\sigma_p^e)[P_p^+(z)+P_p^-(z)] + \frac{1}{\tau_2} + \left(\frac{\Gamma_s}{h\upsilon_s A}\right)(\sigma_s^a+\sigma_s^e)[P_s^+(z)+P_s^-(z)]} \tag{8}$$

$$\Delta n_{core}\left[\Delta T_{core}(r,z), N_2, P_p\right] = \Delta n_{core}\left[\Delta T_{core}(r,z)\right] + \Delta n_{core}\left[N_2(z)\right] + \Delta n_{core}\left[P_p(z)\right] \tag{12}$$

$$\Delta n_{clad}\left[\Delta T_{clad}(r,z), N_2, P_p\right] = \Delta n_{clad}\left[\Delta T_{clad}(r,z)\right] + \Delta n_{clad}\left[N_2(z)\right] + \Delta n_{clad}\left[P_p(z)\right] \tag{13}$$

TABLE II
VARIATION OF THE REFRACTIVE INDEX INSIDE THE FIBER

$r(\mu m)$	$\Delta nT(r,z)[10^{-4}]$	$\Delta n\,(N_2)$	$\Delta nP_p(z)$
1	3.008	4.152μ	2.405μ
5-10	3.007		
15	3.005		
20	3.004		
$r(\mu m)$	$\Delta nT(r,z)[10^{-4}]$	$\Delta n\,(N_2)$	$\Delta nP_p(z)$
25	2.976	0	0
30	2.974		
35	2.973		
40	2.972		
45	2.971		
50	2.970		
100	2.964		
150	2.960		
200	2.958		
250	2.956		
300	2.954		
350	2.953		
400	2.952		

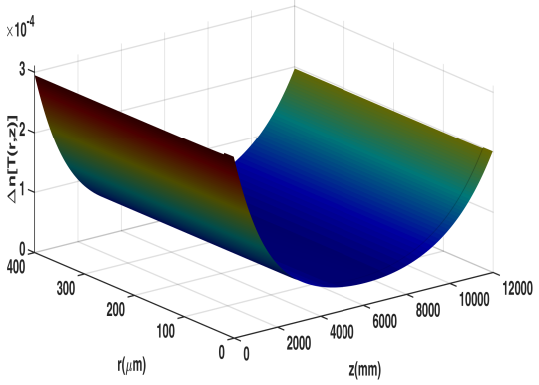

Fig. 1. Profile of the refractive index as a function of $\Delta T(r,z)$.

In Table II and Fig. 2 shown the refractive index changes as a function of the upper-level atomic population density. The changes occur only in the axial direction and in the fiber core with a magnitude of order 4.152×10^{-6} (at the center of the fiber, $z = 0$ and $r \approx 0$).

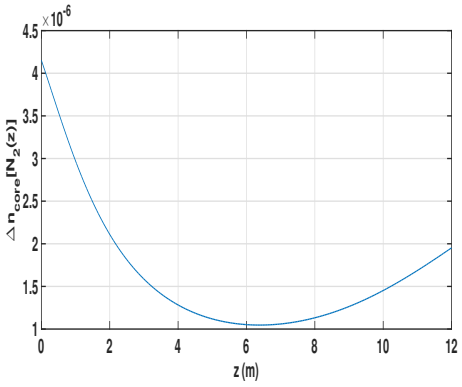

Fig. 2. Longitudinal profile of the refractive index as a function of $N_2(z)$.

According to Table II and Fig. 3, the refractive index changes as a function of the pumping signal occur only in the longitudinal direction and in the core. The minimum occurs at $(L/2)$, and the maxima at the fiber extremities, in the order 2.402×10^{-6} to 2.405×10^{-6}, respectively. Figure 4 presents a profile of the pump signal in the two-end pump mode.

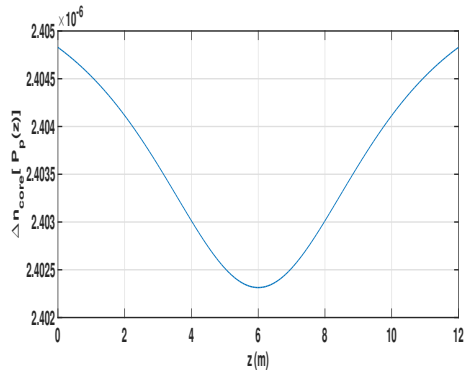

Fig. 3. Longitudinal profile of the refractive index as a function of $P_p\,(z)$.

Moreover, according to Fig. 5 and Table III, the refractive index changes due to wavelength variations of the laser and pumping signals. This effect occurs because of its relationship with the quantum efficiency $S = \frac{\lambda_s}{\lambda_p}$. The values of λ_s and λ_p are the same used by other authors [1, 3, 7], and $N_2(z)$

maintained a variation according to the expected values, from $8.77 \times 10^{23} m^{-3}$ to $3.46 \times 10^{24} m^{-3}$.

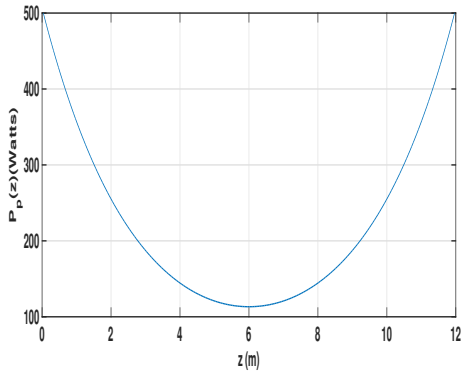

Fig. 4. Longitudinal profile of the pump signal in two-end pump mode.

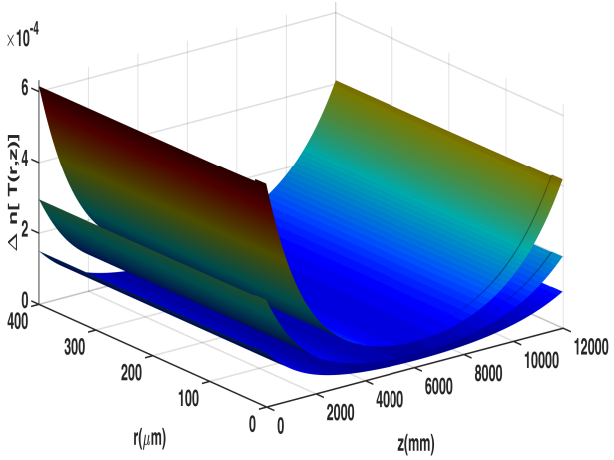

Fig. 5. $\Delta n\left[T(r,z)\right]$ for different values of λ_s and λ_p.

TABLE III
$\Delta n\left[T(r,z)\right]$ DUE TO CHANGES IN λ_s/λ_p

$\boldsymbol{\lambda_s}$	$\boldsymbol{\lambda_p}$	$\boldsymbol{\Delta n\left[T(r,z)\right]}$
$1090nm$	$920nm$	6.270×10^{-4}
$1060nm$	$976nm$	3.008×10^{-4}
$1018nm$	$976nm$	1.525×10^{-4}

In view of these results, the total refractive index changes due to the three effects, along of the optical fiber, for the core and cladding regions, can be written as (12) and (13). Moreover, the refractive index in the cladding region is not influenced by changes in $N_2(z)$ or $P_p(z)$, so $\Delta n_{clad}\left[N_2(z)\right] = \Delta n_{clad}\left[P_p(z)\right] = 0$. In addition, comparing the refractive index changes at $z = 0$, $z = 6m$ and $z = L = 12m$, caused by $N_2(z)$ and $P_p(z)$, the following result is obtained. $\Delta n_{core}\left[N_2(0)\right] \approx 1.72\Delta n_{core}\left[P_p(0)\right]$, $\Delta n_{core}\left[N_2(6)\right] \approx 0.438\Delta n_{core}\left[P_p(6)\right]$ and $\Delta n_{core}\left[N_2(12)\right] \approx 0.812\Delta n_{core}\left[P_p(12)\right]$. This means that the variations in the refractive index caused by $N_2(z)$ are only greater than the variations caused by $P_p(z)$ at $0 \leq z < 1.603m$. Nevertheless, it is in order of magnitude as $1.502 \times 10^{-6} \sim 4.152 \times 10^{-6}$, and varying only in the axial direction and in the core of the optical fiber. However, the variation in the refractive index caused by temperature is greater in any region of the interior of the fiber when it is compared, individually, with the variations caused by $N_2(z)$ or $P_p(z)$, with a minimum variation $\Delta n\left[T_{clad}(r = 400\mu m, z = 6m)\right] = 3.515 \times 10^{-5}$. In the analyses of $\Delta n\left[T(r,z)\right]$ and $\Delta n\left[N_2(z)\right]$, according to Figs. 1 and 2, it was observed that the profile of the refractive index obeys the same behavior of the physical quantity involved (temperature or upper-level atomic population density). This behavior does not occur for the Δn_{core} caused by $P_p(z)$, which can be seen by comparing Fig. 3 with Fig. 4.

IV. Conclusion

This study showed that changes in the refractive index of optical fiber core-cladding have a stronger dependence on the fiber temperature than on the pumping power or the upper-level laser population density, and, as there were no nonlinear optical effects, it was observed that the absorption coefficient and the refractive index did not undergo any variation due to these effects, since $\Delta\alpha_\alpha(\omega^{'})$ and $\Delta n(\omega)$ are related through the Kramers–Kronig relation [6]. The upper-level laser population density $N_2(z)$, the pump power $P_p(z)$, and the signal power $P_s(z)$ remained within the expected range in the axial direction of the optical fiber.

References

[1] M. Peysokhan, E. Mobini, and A. Mafi, "Analytical formulation of a high-power Yb-doped double-cladding fiber laser" OSA Continuum 3, 1940-1951 (2020).

[2] M. Karimi, "Theoretical Study of the Thermal Distribution in Yb-Doped Double-Clad Fiber Laser by Considering Different Heat Sources", Prog. Electromagn. Res., v. 88, p. 59–76, 2018.

[3] J. Li, K. Duan, Y. Wang, X. Cao, W. Zhao, Y. Guo and X. Lin (2008) "Theoretical analysis of the heat dissipation mechanism in Yb^{3+}-doped double-clad fiber Lasers", J. Mod. Opt., 459-471.

[4] P. Yan, "Beam Transmission Properties in High Power Ytterbium-Doped Tandem-Pumping Fiber Amplifier" in IEEE Photonics J., vol. 11, no. 2, pp. 1-12, April 2019, Art no. 1501612.

[5] A. V. Smith and J. J. Smith, "Mode instability in high power fiber amplifiers" AS-Photonics, LLC, 8500 Menaul Blvd. NE, Suite B335, Albuquerque, NM 87112, USA.

[6] M. J. F. Digonnet, R. W. Sadowski, H. J. Shaw, and R. H. Pantell, "Resonantly enhanced nonlinearity in doped fibers for low-power all-optical switching: A review" Opt. Fiber Technol., vol. 3, pp. 44–64, 1997.

[7] P. Yan, "A 1150-W 1018-nm Fiber Laser Bidirectional Pumped by Wavelength-Stabilized Laser Diodes" in IEEE J. Sel. Top. Quantum Electron., vol. 24, no. 3, pp. 1-6, May-June 2018, Art no. 0902506.